nature photonics

LETTERS

https://doi.org/10.1038/s41566-021-00888-7

Check for updates

Intense few-cycle visible pulses directly generated via nonlinear fibre mode mixing

R. Piccoli[1,7]✉, J. M. Brown[2,3,8], Y.-G. Jeong[1], A. Rovere[1], L. Zanotto[1], M. B. Gaarde[3], F. Légaré[1], A. Couairon[2], J. C. Travers[4], R. Morandotti[1,5], B. E. Schmidt[6]✉ and L. Razzari[1]✉

Extremely short, high-energy pulses are essential in modern ultrafast science. In a seminal paper in 1996[1], Nisoli and co-workers demonstrated the first intense pulse compression employing a gas-filled hollow-core fibre. Despite the huge body of scientific work on this technology stemming from ultrafast and attosecond research, here we identify an unexplored few-cycle visible-light generation mechanism, which relies on the nonlinear mixing of hollow-core fibre modes. Using a commercially available ytterbium laser, we generate 4.6 fs, 20 μJ pulses centred at around 600 nm (~2 cycles, ~4 GW peak power), ~40 times shorter than the input 175 fs, 1 mJ pulses at 1,035 nm. Our approach thus directly projects few-hundred-femtosecond-long infrared pulses into the single-cycle regime at visible frequencies, without the need for additional post-compression. As a powerful application of our findings, we present a compact, multicolour pump–probe set-up with a temporal resolution of a few optical cycles.

High-energy pulsed lasers have enabled unprecedented capabilities in driving, controlling and probing ultrafast matter dynamics and nowadays represent the cornerstone of a multitude of research fields such as femtochemistry[2], two-dimensional ultrafast spectroscopy[3], attosecond pulse generation[4] and laser-driven particle acceleration[5]. More specifically, ultrashort visible pulses are essential to temporally resolve ultrafast primary biological processes at the basis of our own existence, including energy transfer between chromophores (related to photosynthesis)[6] and isomerization of rhodopsin (related to human vision)[7], as well as to study the dynamics of photogenerated charges and excitons in semiconductors for next-generation optoelectronic devices[8]. In a pioneering work dating back to the late 1980s, nanojoule-level visible (VIS; central wavelength between 500 and 650 nm) pulses as short as 6 fs were obtained using a femtosecond dye laser followed by additional amplification and pulse compression stages[9]. In spite of this result, dye-based technology was mostly abandoned in the early 1990s in favour of the emerging solid-state neodymium-, Ti:sapphire- and subsequent ytterbium-based systems emitting at 1,064, 800 and 1,030 nm, respectively. The rapid energy upscaling of these systems led—a decade later—to a new compression technique based on the laser spectral broadening in gas-filled hollow-core fibres (HCFs)[1], which nowadays brings high-energy (millijoule-level) optical pulses into the few-cycle regime[10–16]. Nevertheless, the conversion of such pulses in different spectral regions, such as the VIS, still represents a great challenge due to the intrinsic difficulty in managing chromatic dispersion and strong nonlinearities over broad bandwidths. Few-cycle (sub-10-fs) VIS pulses at the microjoule level have so far only been achieved using complex arrangements, mostly based on non-collinear optical parametric amplification[17–19] or optical parametric chirped pulse amplification[20]. Typically, in these schemes, the pump wavelength is the second or third harmonic of the input laser, and some dispersion compensation mechanism (exploiting prisms, gratings, chirped mirrors, etc.) is required to post-compress the generated VIS light in time. Alternative approaches employing gas-filled HCFs rely on the spectral filtering of super-continuum generation[4], resonant dispersive wave emission[21,22], spectral broadening of laser second harmonic[23] or white-light continuum generation via induced-phase modulation[24]; yet, they necessitate a post-compression stage and/or the use of very short input pulses of about 30 fs. Furthermore, a large number of white-light generation mechanisms have been identified over the last half century, in solids, liquids, gases and many different types of fibre[25,26]. Yet, the complex interplay among the involved nonlinear phenomena (for example, self-phase modulation (SPM), cross-phase modulation (XPM), self-focusing, stimulated Raman, ionization, etc.) does not automatically deliver a well-defined temporal pulse in the single-cycle regime.

Inspired by recent pioneering works on nonlinear phenomena in multimode glass fibres[27,28], here we show how all the above challenges can be overcome by abandoning the paradigm that a capillary-type HCF is only useful if it is capable of supporting a single spatial mode. Indeed, the often neglected multimode nature of gas-filled HCFs[29], as well as their very low nonlinearity and dispersion over long propagation distances (metres), gives rise to a unique waveguiding environment for the exploration of unprecedented nonlinear optical dynamics. By exploiting this platform, we achieve the direct generation of high-energy two-cycle VIS pulses with excellent spatiotemporal properties. These are generated from much longer (175 fs) infrared pulses emitted by a commercially available amplified ytterbium laser system.

The experimental realization of this scheme employs 175-fs-long pulses centred at 1,035 nm, which are coupled into a 3-m-long Ar-filled HCF (Fig. 1a). The total transmitted power stands almost constant at 70% up to approximately 0.8 mJ input pulse energy and 3.3 bar gas pressure (Fig. 1b). Experimental evidence of VIS light generation is gained by monitoring the total amount

[1]Institut National de la Recherche Scientifique, Centre Énergie Matériaux Télécommunications (INRS-EMT), Varennes, Québec, Canada. [2]Centre de Physique Théorique, CNRS, Ecole Polytechnique, Institut Polytechnique de Paris, Palaiseau, France. [3]Department of Physics & Astronomy, Louisiana State University, Baton Rouge, LA, USA. [4]School of Engineering and Physical Sciences, Heriot-Watt University, Edinburgh, UK. [5]IFFS, University of Electronic Science and Technology of China, Chengdu, China. [6]few-cycle Inc., Varennes, Québec, Canada. [7]Present address: Department of Physics of Complex Systems, Weizmann Institute of Science, Rehovot, Israel. [8]Present address: Department of Computer Science, Wisconsin Lutheran College, Milwaukee, WI, USA. ✉e-mail: riccardo.piccoli@weizmann.ac.il; schmidt@few-cycle.com; luca.razzari@inrs.ca

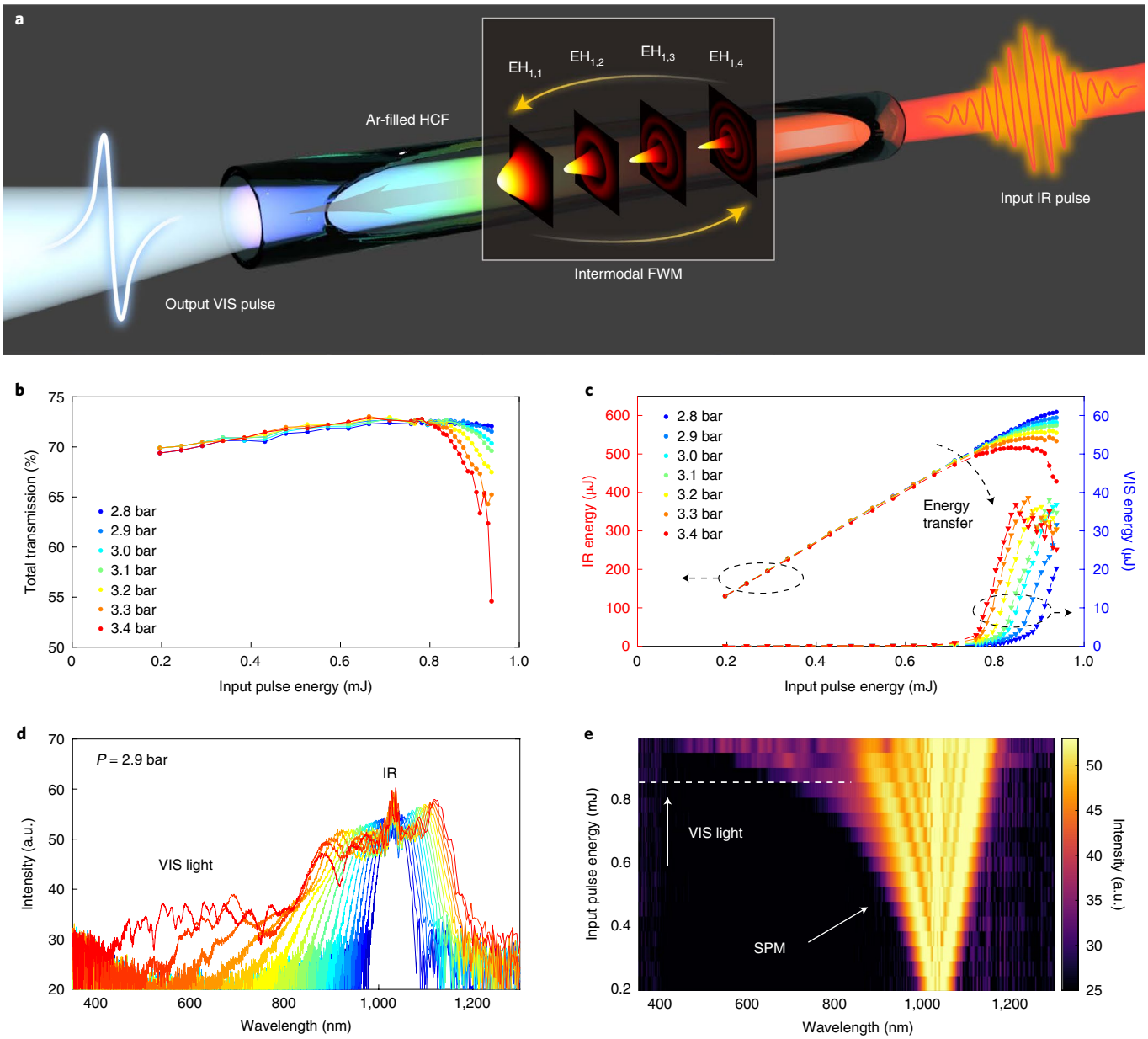

Fig. 1 | Sketch of the generation mechanism, output energy and spectra. a, VIS pulse generation mechanism in the Ar-filled HCF. The spatial intensity profile of modes $EH_{1,n}$ (n = 1, 2, 3, 4) are illustrated in the inset. **b**, Total power transmission through the fibre as a function of the input pulse energy and gas pressure (P). **c**, Transmitted energy in the IR region above 800 nm (left axis) and in the VIS region below 800 nm (right axis). **d**,**e**, Experimental output spectra at 2.9 bar on a decibel scale, as the input pulse energy varies from 0.19 mJ (blue) to 0.94 mJ (red) in steps of approximately 50 μJ. The dashed horizontal line in **e** indicates the onset of VIS light generation.

of output energy located in the two relevant spectral regions, namely, the VIS (400–800 nm) and infrared (IR; 800–1,200 nm) regions; Supplementary Fig. 2 shows a sketch of the experimental set-up. Before ionization takes place, a fast-growing energy transfer between the SPM-broadened IR radiation and the arising VIS light occurs at around 0.8 mJ laser pulse energy (Fig. 1c). A maximum VIS energy of 40 μJ can be generated, corresponding to a conversion efficiency of ~4% with respect to the input pulse energy, which is comparable to the state-of-the-art technology[17–24]. We also recorded the output spectra at different gas pressures and for different input pulse energies. Figure 1d,e illustrates the representative output spectra (on a decibel scale) recorded at 2.9 bar (that is, when the VIS pulse arises) as the input pulse energy varies from 0.19 to 0.94 mJ. For input pulse energies lower than 0.8 mJ (~4.4 GW input peak power), the spectral broadening is mainly dominated by SPM, until suddenly—as the energy overcomes this threshold—a broad VIS light pedestal extending down to 400 nm appears. At this pressure, the critical power for self-focusing is about 5.5 GW, only ~10% higher than the maximum input peak power of 5.0 GW (at 0.94 mJ). This hints at the need for providing enough nonlinearity to effectively transfer energy to higher-order modes through four-wave mixing (FWM), in a sort of discrete form of self-focusing. Although the full nonlinear spatiotemporal dynamics is rather complicated to visualize, the underlying generation mechanism can be condensed into the following intuitive picture. First, higher-order modes are populated via intermodal FWM along the propagation direction, where the (small) phase mismatch between their different propagation constants periodically reverses the FWM gain, thus leading

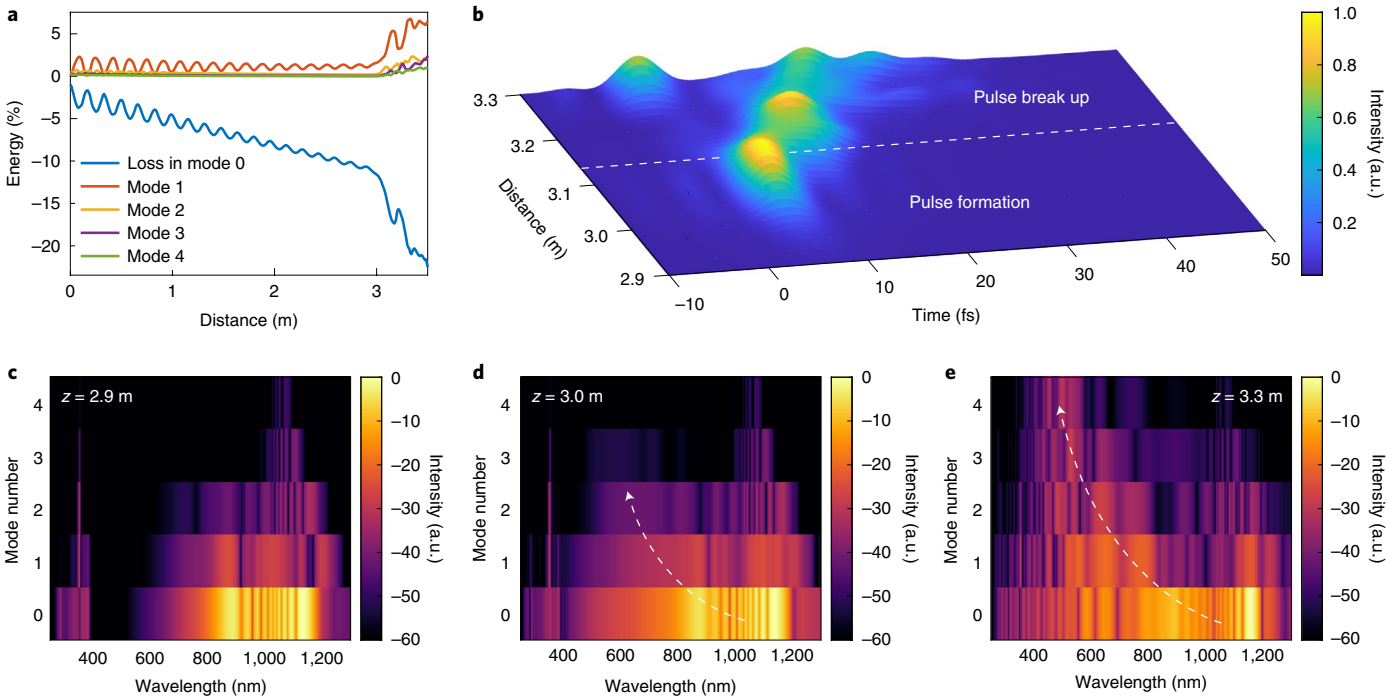

Fig. 2 | VIS pulse formation. a, Energy contained in each mode along the propagation extracted from the numerical simulations. **b**, Simulation regarding the formation and propagation of the VIS pulse in the last portion of the fibre from 2.9 to 3.3 m. A well-defined VIS pulse, obtained by filtering the spectrum from 525 to 750 nm, suddenly appears at around 3.0 m of propagation. After its formation, the pulse quickly breaks up if propagation continues for more than 10–20 cm. **c**, Modally resolved spectrum at $z = 2.9$ m on a decibel scale. SPM around the central laser wavelength and the third harmonic at approximately 345 nm can be clearly observed, while the VIS region is not yet substantially occupied. Both IR laser light and third harmonic are mostly confined in the fundamental mode ($m = 0$). **d**, Modally resolved spectra at $z = 3.0$ m, where a well-defined VIS pulse is generated. In the short span between 2.9 and 3.0 m, the laser energy is rapidly transferred (white dashed arrow) to the first few modes (0, 1 and 2) and homogeneously fills the VIS region. **e**, Modally resolved spectrum at $z = 3.3$ m. A continuous transfer of energy occurs and populates even modes of higher order (3 and 4) with a further expansion into the VIS–ultraviolet region. The spectral fringes indicate disruptive mixing and interference within the modes, consistent with the observation of pulse break-up.

to a continuous exchange of energy between the fundamental and higher-order modes at every coherence length (Supplementary Fig. 1a). Second, new frequencies are also continuously generated via intramodal SPM and intermodal XPM. Because higher-order modes travel with (slightly) lower group velocities than the fundamental mode (Supplementary Fig. 1b), different modes temporally slide over each other during propagation. The 'blue' components in the trailing edge of the faster fundamental mode temporally slide over the 'red' components in the leading edge of the slower higher-order modes, thus generating light towards the VIS domain via FWM.

The intuitive physical mechanism presented above stems from three-dimensional carrier-resolved pulse propagation simulations based on guided mode theory (Supplementary Information). The sources of nonlinearity include the Kerr effect as well as plasma effects due to ionization. We considered up to five fibre modes ($EH_{1,1,\ldots5}$, labelled for simplicity from 0 to 4) as we numerically observed that additional modes do not substantially contribute to VIS light generation. Figure 2a illustrates the energy content in each mode along propagation. As it is possible to observe, there is a clear, periodic energy exchange between the fundamental mode ('loss in mode 0' represents the energy in mode 0 minus the total energy) and the higher-order modes with a half-period of about 8 cm, which is consistent with the theoretical coherence length between mode 0 and mode 1 ($l_c^{(0,1)} = \pi / \left| k_{1035}^{(0)} - k_{1035}^{(1)} \right| \approx 9.6$ cm at Ar gas pressure of 3 bar, $k_\lambda^{(m)}$ being the wavevector of mode m at wavelength λ (ref. [29]); $m = 0$ for the fundamental mode). As the temporal walk-off between the modes increases during propagation, the energy channelled into higher-order modes cannot fully come back into the fundamental mode. Right before 3 m of propagation, where the VIS pulse is formed, there is a clear and notable exchange of energy towards the higher-order modes, which eventually leaves about 5% of the total energy in mode 1. Figure 2b shows the temporal evolution of the generated VIS pulse along propagation, obtained by performing the Fourier transform of the portion of the spectrum located between 525 and 750 nm and integrating along the HCF cross section at a pressure of 3.3 bar. Figure 2c–e shows the modally resolved spectra for three representative distances from the fibre input: $z = 2.9$, 3.0 and 3.3 m. At $z = 2.9$ m, no well-defined VIS pulse has yet formed and there is evidence of SPM and the generation of the third harmonic (Fig. 2c). Within another 10 cm of propagation, there is an observable transfer of energy towards the VIS spectral region mainly involving the first three modes of the fibre (Fig. 2d) and a temporally short pulse appears (Fig. 2b). As propagation continues, phase mismatch between the modes accumulates; after ~3.15 m of propagation, the VIS pulse breaks up (refer to the spectral fringes for $z = 3.3$ m; Fig. 2e). Using the analysis detailed in ref. [30], it is found that the Kerr effect is the dominant nonlinear source in mediating this transfer of energy, while plasma effects due to ionization appear to have little impact on the spectral content of the modes (Supplementary Fig. 20). Therefore, we can conclude that within a specific range of gas pressures and pulse peak intensities, the chromatic and modal dispersions as well as Kerr energy transfer create unique conditions for a few-cycle VIS pulse to occur right before the exit of the fibre, thus being readily available for use. It is worth stressing that multimode propagation is essential to effectively

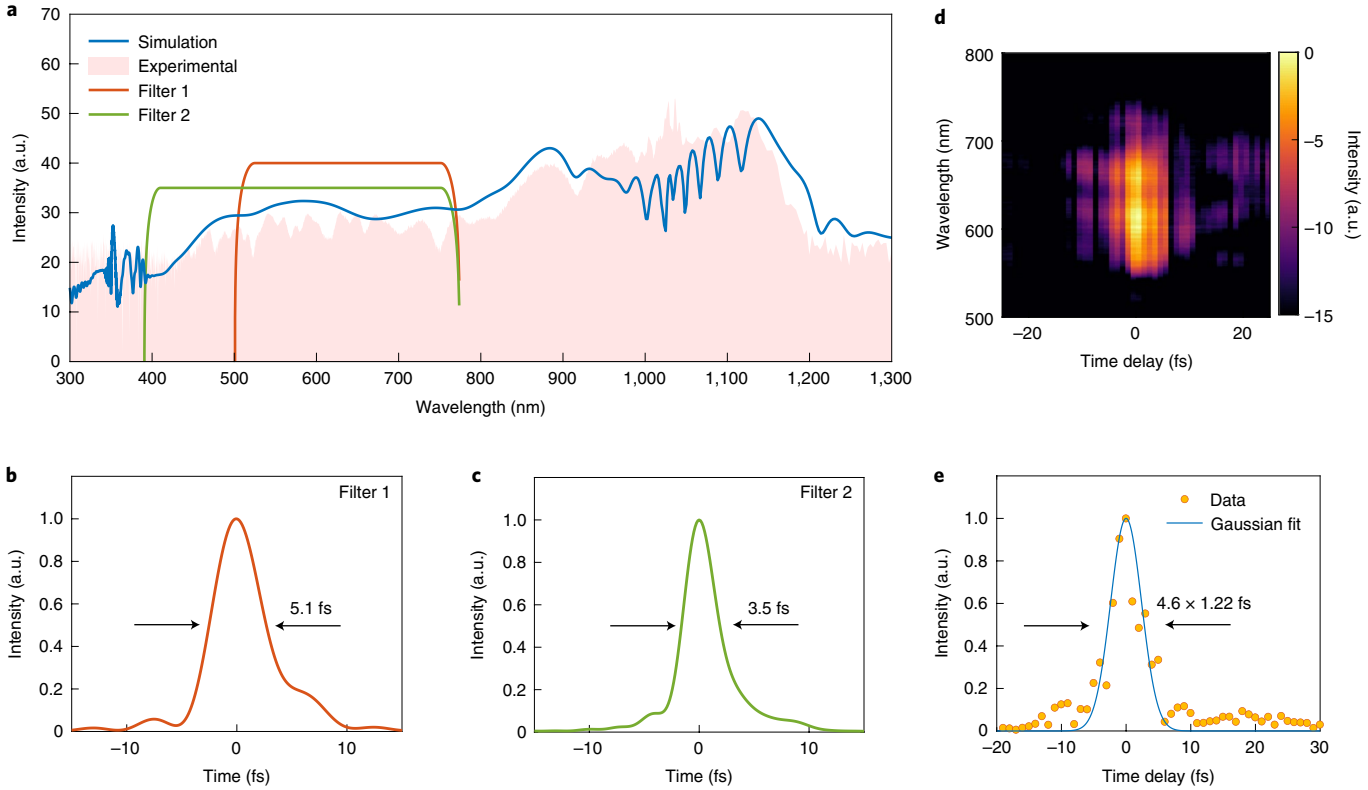

Fig. 3 | Comparison between numerical and experimental results. a, Numerically calculated (3.3 bar and 3.08 m, blue line) and experimental (2.9 bar and 3.00 m, shaded area) output spectra on a decibel scale for an input pulse energy of 0.94 mJ. The orange and green lines represent the filtering functions applied to the numerical results. **b**,**c**, Corresponding temporal pulse intensities calculated by taking the Fourier transform of the spectrum (amplitude and phase) after filter 1 (orange) (**b**) or filter 2 (green) (**c**). **d**,**e**, Measured TG-FROG spectrogram on a decibel colour scale (**d**) and corresponding autocorrelation trace at 2.9 bar gas pressure, returning a pulse duration of 4.6 fs (considering a deconvolution factor of 1.22 for TG-FROG) (**e**).

generate this VIS pulse. Indeed, simulations show that by switching off the higher-order modes at $z = 2.8$ m, VIS light generation is strongly suppressed (see section 2.3 in Supplementary Information).

Figure 3a shows that the output spectrum obtained by our numerical simulations for a gas pressure of 3.3 bar (blue line) is in good agreement with the experimental result (light-red-filled area) at 2.9 bar. Moreover, by filtering the simulated spectrum (while retaining its amplitude and phase) from 750 to 525 nm (filter 1) or from 750 to 400 nm (filter 2), a corresponding transform-limited pulse of 5.1 fs and ~2.4 cycles (Fig. 3b) or 3.5 fs and ~1.8 cycles (Fig. 3c), respectively, is obtained. To experimentally measure the VIS pulse duration, we employed an octave-spanning, dispersion-free, transient-grating frequency-resolved optical gating (TG-FROG) set-up (Methods and Supplementary Figs. 3 and 4). To filter out the IR portion of the output light, we used a calibrated 4f set-up (Supplementary Figs. 13 and 14). The recorded TG-FROG spectrogram is shown in Fig. 3d and the corresponding autocorrelation trace is shown in Fig. 3e (obtained by integrating the spectrogram along the wavelength axis). Within a narrow range of gas pressures (2.9–3.1 bar) and at the maximum pulse energy (0.94 mJ), an ~5-fs-long pulse could be measured. The formation of this VIS pulse shows high reproducibility and stability (with a photodiode, we estimated a standard deviation normalized to the peak amplitude of $\sigma_{white} \approx 1.5\%$ and $\sigma_{laser} \approx 1.2\%$), as well as good beam quality, spatial uniformity and lack of appreciable spatial chirp (Supplementary Figs. 7–10). To rule out the presence of a coherent artefact[31] in our measurement, we additionally performed cross-correlation transient-grating cross-correlation frequency-resolved optical gating (TG-XFROG) between the independently compressed IR laser pulses at the fundamental wavelength and VIS pulses (Methods and Supplementary Fig. 5). We used a pair of broadband chirped mirrors to compress (down to ~3 cycles) the SPM-broadened IR portion of the spectrum, which was reflected in the zero order of the grating employed in the 4f set-up (Fig. 4a). First, via second harmonic generation frequency-resolved optical gating (SHG-FROG) and TG-FROG, we separately characterized the compressed IR pulses and the VIS pulses emerging from the set-up, respectively. Figure 4b,c shows the autocorrelation traces corresponding to a 10 fs IR pulse centred at 1,035 nm and a 7.3 fs VIS pulse centred at around 600 nm. The VIS pulse duration, in this case, was not perfectly optimized since in this specific experiment, we focused on obtaining the proper amount of SPM broadening to optimally compress the IR laser pulses. We then combined three beams—the generated VIS beam with two beams from the compressed IR laser—to perform the TG-XFROG measurements. The result of this procedure, as shown in Fig. 4d, yields a cross-correlation trace of 16.5 fs (full-width at half-maximum), clearly proving the existence of an ultrashort VIS pulse. In addition, the proposed characterization remarkably demonstrates the possibility of directly implementing a high-energy IR pump/VIS probe set-up on a sub-10-fs scale via a single HCF, without the need for any additional complex apparatus.

In conclusion, we have presented a novel mechanism—based on nonlinear mixing between the spatial modes of an HCF—to generate high-quality, high-energy (20 μJ), two-cycle (~4.6 fs) VIS pulses. Starting with 175-fs-long IR laser pulses, ~40 times shorter VIS pulses are directly obtained without the need for any post-compression technique or optical parametric amplification system. In addition, our approach does not alter the conventional SPM broadening of the input laser pulses, which can be independently compressed below 10 fs, thus readily delivering two few-cycle

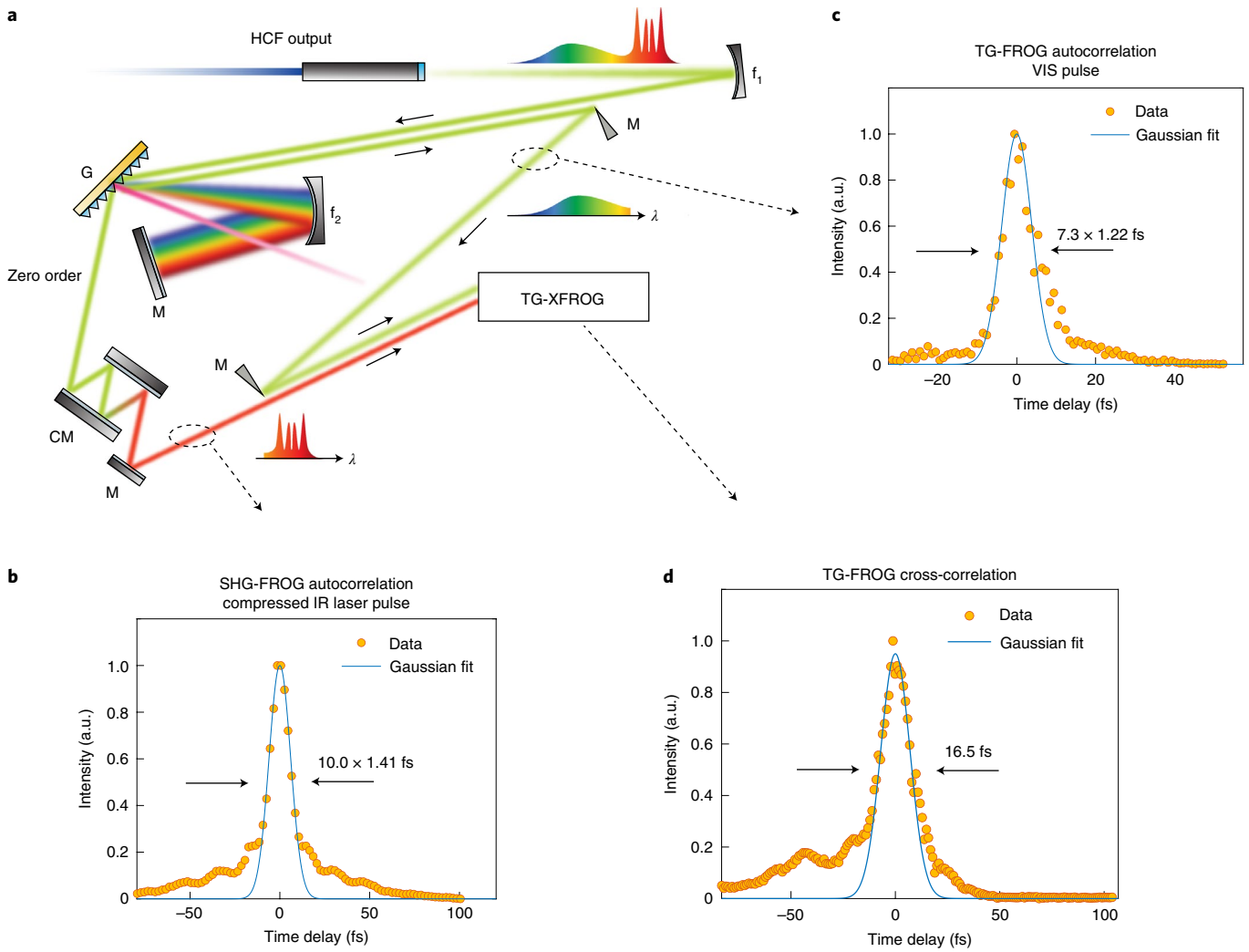

Fig. 4 | Few-cycle IR pump/VIS probe set-up. a, Sketch of the experimental set-up. The output spectrum from the HCF is sent into a 4f set-up to separate the VIS light below 800 nm and the SPM-modulated laser light above 800 nm. The residual SPM-modulated laser light emerging from the zero order of the grating (G) is compressed through a pair of chirped mirrors (CM). The M labels represent metallic plane mirrors, f_1 and f_2 are metallic concave mirrors, and λ is the wavelength. **b**, SHG-FROG autocorrelation trace of the compressed IR laser pulses. **c**, TG-FROG autocorrelation trace of the VIS pulses emerging from the 4f set-up. **d**, TG-FROG cross-correlation trace obtained by combining two IR laser pulses (as in **b**) and the VIS pulse (as in **c**) (Supplementary Information provides further details).

pulses, one in the VIS region and the other in the IR region. Besides representing a drastic simplification of the state-of-the-art technology in intense ultrashort VIS light generation, our result may find a variety of applications in ultrafast science, condensed-matter physics and nonlinear optics at large. For example, it can be used to unveil photoinduced electron transfer processes in organic molecules as well as exciton relaxation dynamics in low-dimensional semiconductors at the few-cycle timescale—investigations of great relevance for applications in photovoltaics and nanoelectronics, respectively[32]. Furthermore, we envision the possibility of scaling up the system to unprecedented VIS-light average powers of tens of watts by efficiently harvesting the high repetition rate potential of the emerging high-power ytterbium-based laser technology[33,34].

Online content

Any methods, additional references, Nature Research reporting summaries, source data, extended data, supplementary information, acknowledgements, peer review information; details of author contributions and competing interests; and statements of data and code availability are available at https://doi.org/10.1038/s41566-021-00888-7.

Received: 4 August 2020; Accepted: 27 August 2021;
Published online: 28 October 2021

References

1. Nisoli, M. et al. Generation of high energy 10 fs pulses by a new pulse compression technique. *Appl. Phys. Lett.* **68**, 2793–2795 (1996).
2. Zewail, A. H. Laser femtochemistry. *Science* **242**, 1645–1653 (1988).
3. Oliver, T. A. A. Recent advances in multidimensional ultrafast spectroscopy. *R. Soc. Open Sci.* **5**, 171425 (2018).
4. Wirth, A. et al. Synthesized light transients. *Science* **334**, 195–200 (2011).
5. Hooker, S. M. Developments in laser-driven plasma accelerators. *Nat. Photon.* **7**, 775–782 (2013).
6. Cerullo, G. et al. Photosynthetic light harvesting by carotenoids: detection of an intermediate excited state. *Science* **298**, 2395–2398 (2002).
7. Schoenlein, R. W. et al. The first step in vision: femtosecond isomerization of rhodopsin. *Science* **254**, 412–415 (1991).

8. Chemla, D. S. & Shah, J. Many-body and correlation effects in semiconductors. *Nature* **411**, 549–557 (2001).
9. Fork, R. L. et al. Compression of optical pulses to six femtoseconds by using cubic phase compensation. *Opt. Lett.* **12**, 483–485 (1987).
10. Bohman, S. et al. Generation of 5.0fs, 5.0mJ pulses at 1kHz using hollow-fiber pulse compression. *Opt. Lett.* **35**, 1887–1889 (2010).
11. Jeong, Y.-G. et al. Direct compression of 170-fs 50-cycle pulses down to 1.5 cycles with 70% transmission. *Sci. Rep.* **8**, 11794 (2018).
12. Nisoli, M. et al. Toward a terawatt-scale sub-10-fs laser technology. *IEEE J. Sel. Topics Quantum Electron.* **4**, 414–419 (1998).
13. Robinson, J. S. et al. The generation of intense, transform-limited laser pulses with tunable duration from 6 to 30 fs in a differentially pumped hollow fibre. *Appl. Phys. B* **85**, 525–529 (2006).
14. Silva, F. et al. Strategies for achieving intense single-cycle pulses with in-line post-compression setups. *Opt. Lett.* **43**, 337–340 (2018).
15. Cardin, V. et al. 0.42 TW 2-cycle pulses at 1.8 µm via hollow-core fiber compression. *Appl. Phys. Lett.* **107**, 181101 (2015).
16. Böhle, F. et al. Compression of CEP-stable multi-mJ laser pulses down to 4 fs in long hollow fibers. *Laser Phys. Lett.* **11**, 095401 (2014).
17. Cerullo, G. et al. Sub-8-fs pulses from an ultrabroadband optical parametric amplifier in the visible. *Opt. Lett.* **23**, 1283–1285 (1998).
18. Baltuška, A. et al. Visible pulse compression to 4 fs by optical parametric amplification and programmable dispersion control. *Opt. Lett.* **27**, 306–308 (2002).
19. Odhner, J. H. & Levis, R. J. High-energy noncollinear optical parametric amplifier producing 4 fs pulses in the visible seeded by a gas-phase filament. *Opt. Lett.* **40**, 3814–3817 (2015).
20. Harth, A. et al. Two-color pumped OPCPA system emitting spectra spanning 15 octaves from VIS to NIR. *Opt. Express* **20**, 3076–3081 (2012).
21. Brahms, C. et al. Infrared attosecond field transients and UV to IR few-femtosecond pulses generated by high-energy soliton self-compression. *Phys. Rev. Res.* **2**, 043037 (2020).
22. Travers, J. C. et al. High-energy pulse self-compression and ultraviolet generation through soliton dynamics in hollow capillary fibres. *Nat. Photon.* **13**, 547–554 (2019).
23. Liu, J. et al. Generation of stable sub-10 fs pulses at 400 nm in a hollow fiber for UV pump-probe experiment. *Opt. Express* **18**, 4664–4672 (2010).
24. Matsubara, E. et al. Generation of 2.6 fs optical pulses using induced-phase modulation in a gas-filled hollow fiber. *J. Opt. Soc. Am. B* **24**, 985–989 (2007).
25. Russell, P. S. J. et al. Hollow-core photonic crystal fibres for gas-based nonlinear optics. *Nat. Photon.* **8**, 278–286 (2014).
26. Alfano, R. R. The Supercontinuum Laser Source: *The Ultimate White Light 2nd edn* (Springer, 2016).
27. Wright, L. G. et al. Controllable spatiotemporal nonlinear effects in multimode fibres. *Nat. Photon.* **9**, 306–310 (2015).
28. Krupa, K. et al. Multimode nonlinear fiber optics, a spatiotemporal avenue. *APL Photonics* **4**, 110901 (2019).
29. Marcatili, E. A. J. & Schmeltzer, R. A. Hollow metallic and dielectric waveguides for long distance optical transmission and lasers. *Bell Syst. Tech. J.* **43**, 1783–1809 (1964).
30. Brown, J. M. et al. Analysis of the angular spectrum for ultrashort laser pulses. *J. Opt. Soc. Am. B* **36**, A105–A111 (2019).
31. Ratner, J. et al. Coherent artifact in modern pulse measurements. *Opt. Lett.* **37**, 2874–2876 (2012).
32. Manzoni, C. et al. Two-color pump-probe system broadly tunable over the visible and the near infrared with sub-30 fs temporal resolution. *Rev. Sci. Instrum.* **77**, 023103 (2006).
33. Schmidt, B. E. et al. Highly stable, 54 mJ Yb-InnoSlab laser platform at 0.5 kW average power. *Opt. Express* **25**, 17549–17555 (2017).
34. Nagy, T. et al. Generation of three-cycle multi-millijoule laser pulses at 318 W average power. *Optica* **6**, 1423–1424 (2019).

Methods

Experimental set-up. We employed a 3-m-long HCF with a 500 µm inner diameter (few-cycle Inc.). Transform-limited 175 fs (full-width at half-maximum) pulses centred at 1,035 nm with an energy of up to 1 mJ and repetition rate of 6 kHz (average power of up to 6 W) were obtained from a Yb:KGW regenerative amplifier (LIGHT CONVERSION). The laser beam was coupled into the fibre through an anti-reflection-coated, 1-mm-thick fused-silica input window. An uncoated, 1-mm-thick fused-silica output window was used instead to enable broadband operation. The output beam was collimated by means of an aluminium-coated concave mirror (f = 1 m) and sent through a series of metallic mirrors into a calibrated 4f set-up to compensate the dispersion accumulated by the VIS pulse from the exit of the fibre to the characterization stage. The 4f set-up was realized in a reflection geometry with a ruled reflective diffraction grating (600 grooves per millimetre blazed at 500 nm; Thorlabs) and a concave aluminium-coated mirror (f = 200 mm; Thorlabs).

Spectral/temporal characterization. The spectrum of the output pulses was measured by combining two different Avantes spectrometers, together covering the region of 300–1,800 nm. The recorded spectra were then corrected by considering the corresponding spectrometer sensitivities, obtained through the measurement of the spectral intensity of a black-body source at a given temperature. The output pulses were characterized via SHG-FROG and TG-FROG (few-cycle Inc.). The set-ups comprise all-reflective optics, a motorized delay stage (Physik Instrumente), and a 10-µm-thick β-barium borate crystal (SHG-FROG) or a 240-µm-thick silica window (TG-FROG). In both cases, the signal is spatially selected and focused into the fibre-coupled spectrometer (Avantes) by means of a CaF_2 lens with 40 mm focal length. The compression of laser pulses for TG-XFROG measurements was obtained via broadband chirped mirrors featuring high-reflectivity between 800 and 1,200 nm (PC1611, UltraFast Innovations), adding some glass windows to finely tune the total group delay dispersion to −480 fs^2.

Data availability

The data that support the plots within this paper and other findings of this study are available from the corresponding authors upon reasonable request.

Code availability

The computer code used in this study is available from the corresponding authors upon reasonable request.

Acknowledgements

We would like to thank Natural Sciences and Engineering Research Council of Canada (NSERC) (Collaborative Research and Development (CRD) and Discovery Grants) and Prompt, Québec. J.M.B. acknowledges support from the Air Force Office of Scientific Research under MURI award no. FA9550-16-1-0013. R.M. is affiliated to IFFS as an adjoint faculty.

Author contributions

R.P. performed the experiments with the support of Y.-G.J., A.R. and L.Z. J.M.B. performed the numerical simulations. A.C., M.B.G. and J.C.T. supervised the numerical simulations. B.E.S. and L.R. conceived the study and supervised its realization. R.M. and F.L. provided technical support. All the authors discussed the experimental results and helped with the preparation of the manuscript.

Competing interests

The authors declare no competing interests.

Additional information

Supplementary information The online version contains supplementary material available at https://doi.org/10.1038/s41566-021-00888-7.

Correspondence and requests for materials should be addressed to R. Piccoli, B. E. Schmidt or L. Razzari.

Peer review information *Nature Photonics* thanks Daniele Faccio and the other, anonymous, reviewer(s) for their contribution to the peer review of this work.